HAL
open science

Nondegenerate Four-Wave Mixing in a Dual-Mode Injection-Locked InAs/InP(100) Nanostructure Laser

Cheng Wang, Frédéric Grillot, Fan-Yi Lin, Ivan Aldaya, Thomas Batte, Christophe Gosset, Etienne Decerle, Jacky Even

To cite this version:

Cheng Wang, Frédéric Grillot, Fan-Yi Lin, Ivan Aldaya, Thomas Batte, et al.. Nondegenerate Four-Wave Mixing in a Dual-Mode Injection-Locked InAs/InP(100) Nanostructure Laser. IEEE Photonics Journal, 2014, 6 (1), pp.1500408. 10.1109/JPHOT.2013.2295473 . hal-00942561

HAL Id: hal-00942561
https://hal.science/hal-00942561v1

Submitted on 11 Mar 2014

HAL is a multi-disciplinary open access archive for the deposit and dissemination of scientific research documents, whether they are published or not. The documents may come from teaching and research institutions in France or abroad, or from public or private research centers.

L'archive ouverte pluridisciplinaire **HAL**, est destinée au dépôt et à la diffusion de documents scientifiques de niveau recherche, publiés ou non, émanant des établissements d'enseignement et de recherche français ou étrangers, des laboratoires publics ou privés.

Nondegenerate four-wave mixing in a dual-mode injection-locked InAs/InP(100) nanostructure laser

Cheng Wang,[1,2] Frédéric Grillot,[1] Fan-Yi Lin[3], Ivan Aldaya,[1,4] Thomas Batte,[2] Christophe Gosset[1], Etienne Decerle,[5] and Jacky Even,[2]

[1]Télécom ParisTech, Ecole Nationale Supérieure des Télécommunications, CNRS LTCI, 46 rue Barrault, 75634 Paris Cedex, France
[2]Université Européenne de Bretagne, Laboratoire CNRS FOTON, INSA, 20, avenue des buttes de Coesmes, 35043 Rennes Cedex, France
[3]Institute of Photonics Technologies, Department of Electrical Engineering, National Tsing Hua University, Hsinchu 300, Taiwan
[4]Instituto Tecnológico y de Estudios Speriores de Monterrey, Monterrey, Mexico
[5]Yenista Optics, 4, rue Louis de Broglie, 22300 Lannion Cedex, France

Corresponding author: Cheng Wang (e-mail: cheng.wang@insa-rennes.fr)

Abstract: The nondegenerate four-wave mixing (NDFWM) characteristics in a quantum dot Fabry-Perot laser are investigated employing the dual-mode injection-locking technique. The solitary laser is featured with two lasing peaks, which provides the possibility for an efficient FWM generation. Under optical injection, the NDFWM is operated up to a detuning range of 1.7 THz with a low injection ratio about 0.42. The normalized conversion efficiency (NCE) and the side-mode suppression ratio (SMSR) with respect to the converted signal are analyzed. The highest NCE of -17 dB associated with a SMSR of 20.3 dB is achieved at a detuning of 110 GHz.

Index Terms: Quantum dot laser, injection locking, four-wave mixing.

1. Introduction

Optical wavelength conversion technique plays an important role in the wavelength division multiplexed (WDM) systems. The NDFWM in semiconductor gain media is a quite favorable source for wavelength conversion due to its ultrafast nature and transparency to the modulation format of the signals [1], [2]. In addition, since the converted signal is the phase-conjugate replica of the input signal, it also provides the possibility for fiber dispersion compensation in long distance transmission systems [3], [4]. NDFWM in semiconductor optical amplifiers (SOAs) and distributed feedback (DFB) lasers have been extensively studied and much effort has been devoted to enhance the conversion efficiency (the ratio of the output-converted signal power to the input-signal power) and the optical signal-to-noise ratio |5]-[9]. Generally, the SOA has a larger linear gain, which provides high conversion efficiency, whereas it also generates an additional amplified spontaneous emission noise. In such way, there is an optimum linear gain for the maximum conversion efficiency to noise ratio [5], while a compromise on the pump-wave power is also required to obtain a better performance [6]. In DFB lasers, the lasing mode itself is used as a pump wave, and the NDFWM is enhanced by the cavity resonance. A higher conversion efficiency associated with a lower noise level can be achieved from a laser with a long cavity and a small grating coupling coefficient. Besides, a high lasing power is also favorable for obtaining higher conversion efficiency [7]-[9]. As for the

nonlinear gain medium, in contrast to the quantum well (QW) material, quantum dots (QDs) offer various advantages such as a wider gain spectrum [10], ultrafast carrier dynamics [11], higher nonlinear gain effect and thus a larger three-order nonlinear susceptibility [9], [12], [13]. In addition, due to the reduced linewidth enhancement factor (LEF), QDs have the possibility of eliminating destructive interference among the nonlinear processes and offering an enhanced efficiency in the wavelength up-conversion [14], [15]. In order to improve the dynamical performance of semiconductor lasers, the optical injection-locking technique has been widely used to reduce the spectral linewidth, frequency chirp as well as to suppress relative intensity noise and nonlinear distortion [16]-[18]. Particularly, it has been reported that the LEF value can be reduced under strong optical injection as well [19]-[21], which is quite beneficial for further suppressing the destructive interference. Employing a dual-mode injection-locking scheme in this work, we report the efficient NDFWM generation in a QD Fabry-Perot (FP) laser, in which one tone of the injected continuous-wave (CW) lights is used as the pump wave, while the other one plays the role of the probe wave. Each of them locks a longitudinal mode of the FP laser within the stable-locking range.

2. Experimental Setup

Figure 1 shows the experimental setup, where two tunable CW lasers ($TL_{1,2}$: Yenista Optics, T100S) are injected into the QD laser via an optical circulator. The QD laser output is collected from port 3 of the circulator, which is followed by a 90/10 fiber splitter. The 10% port is connected with a power meter (PM) to monitor the output power while the 90% port is used to analyze the optical spectrum with an optical spectrum analyzer (OSA). The polarization of the tunable lasers is controlled to align with the slave laser through the polarization controller (PC). The temperature of the QD laser is kept constant at 293 K throughout the experiment using a thermo-electric cooler.

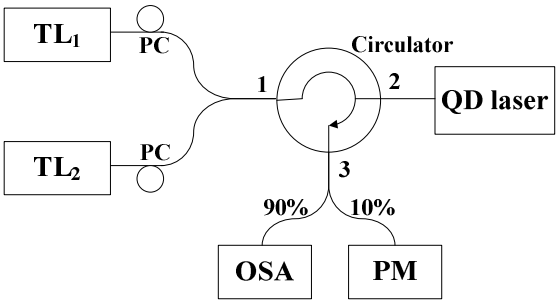

Fig. 1. Schematic of the experimental setup. $TL_{1,2}$: Tunable laser ; PC : Polarization controller ; OSA : Optical spectrum analyzer ; and PM : Power meter.

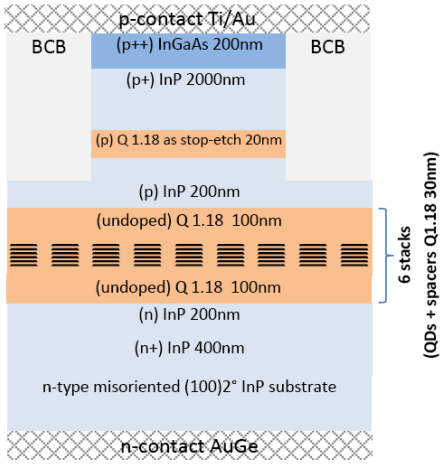

Fig. 2. The epi-layer structure of the InAs/InP(001) QD laser.

Figure 2 illustrates the epi-layer structure of the QD laser. The QD structure was grown by gas source molecular beam epitaxy on a 2° misoriented (100) n-doped InP substrate. The misorientation allows the formation of QDs instead of quantum dashes which are traditionally formed on InP(100) oriented substrate [22]. The active layer consists of six stacked layers of InAs dots which are embedded in an InGaAsP quaternary alloy. The 4-µm wide ridge waveguide was fabricated by selective wet and dry etching sequence based on a CH_4-H_2-Ar RIE plasma using a Ti-Au mask. Then, a benzocyclobutene layer was spin-coated to planarize the mesa structure and dry-etched back to expose the top surface of the ridge. This self-alignment step allows the p-contact electrode by Ti-Au e-beam evaporation. The substrate was thinned to 150 µm and a backside n-type metallization was performed with an AuGe sputtered alloy. Finally, the device was as-cleaved into a 830-µm long cavity.

3. Results and Discussions

Figure 3(a) depicts the output power of the solitary QD laser coupled into a lensed optical fiber as a function of the pump current at room temperature. The laser exhibits a threshold current of about 64 mA. Interestingly, when the current increases above threshold, the free-running optical spectrum is broadened as shown in the inset (green) at 90 mA with a peak centered around 1635 nm, and then splits into two separated peaks above about 98 mA (dashed line). As an illustration, the spectral difference between the split peaks at 110 mA (blue) is 17 nm while it increases up to 23 nm at 160 mA. The phenomenon that the wavelength detuning is varied by the pump current is a specific feature of the QD material and has been already reported in [23]. The corresponding physical mechanism was attributed to the Rabi oscillation as well as to the state filling effect [23], [24]. It is noted that this typical feature observed in the optical spectrum is not contributed from the vertical electronic coupling of the QD multi-layers [25] or the separate excited state emission [26]. The wide split optical spectrum provides the possibility for the efficient generation of wide tuning range NDFWM. Employing the Hakki-Paoli method [27], the extracted net modal gain at the threshold current is shown in Fig. 3(b). The gain spectrum exhibits a full-width at half maximum (FWHM) of about 81 nm and a maximum gain of 14.4 cm^{-1} at 1634.5 nm. Moreover, it has been shown that such a QD laser structure has the capability to reach an even higher material gain [28]. In the experimental study of the NDFWM performance, the QD laser is biased at 110 mA with a fiber-coupled power of 2.0 mW. The powers of the two tunable lasers are both set at around 1.4 mW (1.43 mW for $TL_1$and 1.38 mW TL_2), which are measured at port 2 of the circulator. Assuming a power coupling efficiency of 60% [29], the injection ratio of the master laser to the slave laser is calculated to be 0.42, meaning that the strength of the optical injection remains at a relatively low level. The wavelength of the master laser TL_1 is fixed around the center of peak 1 and acts as the pump wave, while TL_2 is tuned to a longer wavelength and acts as the probe wave.

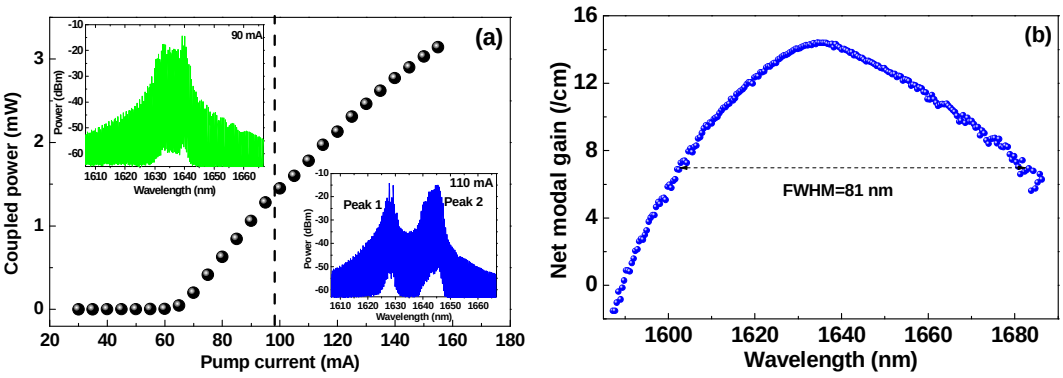

FIG. 3. (a) Light versus pump current, the dashed line indicates the onset of the optical spectrum split. Insets are the free-running spectrums measured at 90 mA (green) and 110 mA (blue), respectively. (b) Net modal gain spectrum at threshold with a FWHM of 81 nm.

Figure 4 shows an optical spectrum in the dual-mode injection-locked QD laser. Each injected light selects a longitudinal mode within the free-running FP multimodes, while other modes are well suppressed. M_1 and M_2 are the stable locked modes by TL_1 and TL_2, respectively. Due to the third-order nonlinear susceptibility $\chi^{(3)}$, new waves S_1 and S_2 are generated as the converted conjugate signal of M_2 and M_1. Assuming the frequency difference between M_1 and M_2 is $\Delta f = f_{M1} - f_{M2}$, the FWM process is governed by the carrier density pulsation (CDP) mechanism for Δf in a few GHz [30], where the beating between the pump and probe waves creates temporal gain and index gratings. For larger frequency detunings up to THz range, the spectral hole burning (SHB) and carrier heating (CH) dominates. In the SHB mechanism, the injected signals create a hole and change the intraband carrier distribution, producing modulation of occupation probability of carriers within the energy band [31]. In the case of QD lasers, the slow interdot processes in a few to tens of picoseconds allow for creating deeper spectral holes and thus for more efficient FWM [11]. The CH mechanism is caused by the stimulated emission from the ground state, which removes the lowest energy carriers while free carriers absorb photons and increase the energy [11], [31]. The frequencies of the two newly generated signals respectively are $f_{S1} = f_{M1} + \Delta f$ and $f_{S2} = f_{M2} - \Delta f$. Then the corresponding susceptibilities are [14]:

$$\begin{aligned} \chi^{(3)}(f_{S_1}) &= \sum_B \chi_B^{(3)}(\Delta f = 0)\left(1 - i2\pi\Delta f\,\tau_B\right)^{-1} \\ \chi^{(3)}(f_{S_2}) &= \sum_B \chi_B^{(3)}(\Delta f = 0)\left(1 + i2\pi\Delta f\,\tau_B\right)^{-1} \end{aligned} \tag{1}$$

where B denotes the contributions from SHB, CH and CDP, τ_B is the corresponding time constant. The electric field of the FWM signal is proportional to the induced polarization [32]:

$$\begin{aligned} \bar{P}(f_{S_1}) &= \varepsilon_0 \chi^{(3)}(f_{S_1}) E^2(f_{M_1}) E^*(f_{M_2}) \\ \bar{P}(f_{S_2}) &= \varepsilon_0 \chi^{(3)}(f_{S_2}) E^2(f_{M_2}) E^*(f_{M_1}) \end{aligned} \tag{2}$$

The normalized conversion efficiency (NCE) is then found to be [33]:

$$\eta_{S1} = \frac{P_{S1}}{P_{M1}^2 P_{M2}}; \quad \eta_{S2} = \frac{P_{S2}}{P_{M2}^2 P_{M1}} \tag{3}$$

where P_X ($X=M_{1,2},S_{1,2}$) is the corresponding wave output power, which can be extracted from the optical spectrum. Following this definition, the normalized conversion efficiency (black) of the FWM in the QD laser is presented in Fig. 5. The interval of the detuning frequency Δf is mainly determined by the mode spacing, which is 0.46 nm in the QD laser under study. The detuning frequency is then operated from the minimum 57.6 GHz up to 1.72 THz. For even larger detunings up to 5.7 THz, the FWM signal is submerged in the residual FP modes or noise and becomes invisible. Due to the asymmetric gain spectrum as shown in Fig. 3(b) and carrier populations in higher energy non-lasing states, the QD laser has a non-zero LEF parameter. By extracting the differential gain and the wavelength drift with the pump current, the measured below-threshold LEF of the laser device under study is found to be 2.6 at 1625 nm. As a result, this finite LEF value makes the susceptibilities $\chi_{CDP}^{(3)}$, $\chi_{SHB}^{(3)}$ and $\chi_{CH}^{(3)}$ in different directions at zero detuning [14]. When the frequency difference is tuned, on one hand $\chi_{CDP}^{(3)}$ begins to rotate and its direction becomes closer to that of $\chi_{SHB}^{(3)}$ and $\chi_{CH}^{(3)}$. On the other hand, the magnitude of each susceptibility becomes smaller as expressed in equation (1). Then η increases and reaches the peak value when the norm of the three additive susceptibilities is the largest. In the experiment under study, this situation is achieved at the detuning frequency Δf =109.6 GHz with a normalized conversion efficiency of -17 dB (η_{S1}). Beyond that, the direction of $\chi_{CDP}^{(3)}$ deviates away and the conversion efficiency decreases with the detuning frequency. When Δf is tuned above the characteristic rates (1 THz) of the SHB and CH

processes, $\chi^{(3)}_{SHB}$ and $\chi^{(3)}_{CH}$ also begin to rotate making η nearly constant at about -34 dB from Δf = 1.13 THz to 1.72 THz in the experiment. It is noted that at a detuning frequency around 1.1 THz, the NCE of the studied QD laser is more than 15 dB larger than that of a QW SOA reported in [33]. From equations (1)-(3), it can be derived that η_{S1}= η_{S2}. However, the experimental results depicted in Fig. 5 shows that η_{S2} is slightly smaller than η_{S1}, which is attributed to that the SHB effect contributes less to the wavelength up-conversion [34]. In addition, Fig. 5 also presents the variation of SMSR (blue) with respect to each converted signal S_1 and S_2 since the residual modes act as optical noise to the converted signals. It decreases with the detuning frequency and the highest SMSR is 20.3 dB at Δf =109.6 GHz. The SMSR of S_2 is smaller in comparison with S_1, which can be partly attributed to the lower power of S_2. On the other hand, the gain at the right side of the pump wave M_1 is larger than that at the left side as shown in Fig. 3(b). Then the amplitude of the residual FP modes at the longer wavelength side is higher when the laser is injection locked.

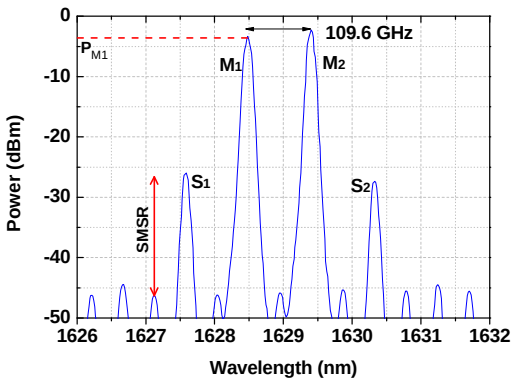

FIG. 4. Optical spectrum with FWM. $M_{1,2}$ are the stably locked modes by the tunable master lasers. The frequency difference between the locked modes is 109.6 GHz. $S_{1,2}$ are the newly converted signals.

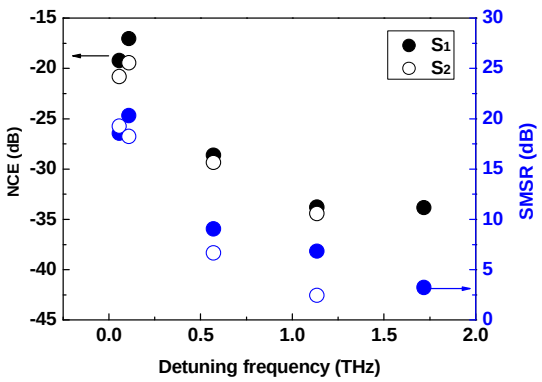

FIG. 5. The normalized conversion efficiency (NCE) η_{S1}, η_{S1} (black) and SMSR (blue) as a function of the detuning frequency. S_1 is denoted by the full circle, and S_2 is by the open circle.

Lastly, it is important to note that in the experiment both the pump wave and the probe signal are operated in the stable-locked regime. However, for an arbitrary probe wavelength in practice, the temperature of the FP laser can be controlled to tune one of the FP modes within the stable-locking range of the probe signal. In addition, because the converted signal is enhanced by the cavity resonance, it is important to make the converted signal located at one resonance frequency peak of the laser cavity [35]. This can be achieved by tuning the pump wave since it typically has a large power and thus a wide locking range. Furthermore, the normalized conversion efficiency can be enhanced by a larger bias current to the FP laser,

since the output power is mainly determined by the slave laser. The SMSR can be improved by a higher injection ratio [35], which can be achieved by coupling an amplifier into the configuration to amplify the pump wave power. Unfortunately, the impact of the injection strength on the FWM was not studied in this work due to the power limitation of the devices, which will be fulfilled in the following work.

4. Conclusion

In conclusion, we have experimentally investigated the NDFWM in a U-band QD FP laser employing the dual-mode injection-locking technique. Taking advantage of the two-peak lasing features of the free-running laser, efficient NDFWM is demonstrated from the 58 GHz detuning up to 1.7 THz under a weak optical injection level. The performance can be further enhanced by increasing the FP laser bias current and by a higher injection ratio of the pump wave, which needs further investigation in the future work. These results are of prime importance for the device applications in the wavelength conversion technique for the future high-speed WDM systems as well as in the microwave signal generation and radio-over-fiber applications in the optical communication networks.

The authors would like to thank Professors Alain Le Corre from INSA-Rennes for providing the QD lasers and Philippe Gallion from Télécom ParisTech for helpful discussions. Dr. Frédéric Grillot's work is supported by the European Office of Aerospace Research and Development (EOARD) under grant number FA8655-12-1-2093. Cheng Wang's work is supported by China Scholarship Council.

References

[1] M. C. Tatham, G. Sherlock, and L. D. Westbrook, "20-nm optical wavelength conversion using nondegenerate four-wave mixing," IEEE Phonon. Technol. Lett., vol. 5, no. 11, pp. 1303-1306, Nov. 1993.

[2] D. F. Geraghty, R. B. Lee, M. Verdiell, M. Ziari, A. Mathur, and K. J. Vahala, "Wavelength conversion for WDM communication systems using four-wave mixing in semiconductor optical amplifiers," IEEE J. sel. Top. Quantum. Electron., vol. 3, no. 5, pp. 1146-1155, Oct. 1997.

[3] M. C. Tatham, X. Gu, L. D. Westbrook, G. Sherlock and D. M. Spirit, "Transmission of 10 Gbit/s directly modulated DFB signals over 200 km standard fibre using mid-span spectral inversion," Electron. Lett., vol. 30, no. 16, pp. 1335-1336, Aug.1994.

[4] D. D. Marcenac, D. Nesset, A. E. Kelly, M. Brierly A. D. Elllis, D. G. Moodie, and C. W. Ford, "40 Gbit/s transmission over 406 km of NDSF using mid-span spectral inversion by four-wave mixing in a 2 mm long semiconductor optical amplifier," Electon. Lett., vol. 33, no. 10, pp. 879-880, May. 1997.

[5] H. J. Kim, H. J. Song, and J. I. Song, "All-optical frequency up-conversion technique using four-wave mixing in semiconductor optical amplifiers for radio-over-fiber applications," Microwave Symposium. IEEE/MTT-S International, pp. 67-70, Jun. 2007.

[6] A. D'Ottavi, F. Martelli, P. Spano, A. Mecozzi, S. Scotti, R. D'Ara, J. Eckner, and G. Guekos,"Very high efficiency fourwave mixing in a single semiconductor traveling wave amplifier," Appl. Phys. Lett., vol. 68, no.16, pp. 2186-2188, Apr. 1996.

[7] T. Simoyama, H. Kuwatsuka, H. Ishikawa, "Cavity length dependence of wavelength conversion efficiency of four-wave mixing in λ/4-shifted DFB laser," FUJISU Sci. Tech. J., vol. 34, no. 2, pp. 235-244, Dec. 1998.

[8] H. J. Kim, and J. I. Song, "All-optical frequency downconversion technique utilizing a four-wave mixing effect in a single semiconductor optical amplifier for wavelength division multiplexing radio-over-fiber applications," Optics Express, vol. 20, no. 7, pp. 8047-8054, Mar. 2012.

[9] H. Su, H. Li, L. Zhang, Z. Zou A. L. Gray, R. Wang, P. M. Varangis, and L. F. Lester, "Nondegenerate four-wave mixing in quantum dot distributed feedback lasers," IEEE Phonon. Technol. Lett., vol. 17, no. 8, pp. 1686-1688, Aug. 2005.

[10] H. Li, G. T. Liu, P. M. Varangis, T. C. Newell, A. Stintz, B. Fuchs, K. J. Malloy, and L. F. Lester, "150-nm tuning range in a grating-coupled external cavity quantum-dot laser," IEEE Photon. Technol. Lett., vol. 12, no. 7, pp. 759-761, Jul. 2000.

[11] D. Nielsen, and S. L. Chuang, "Four-wave mixing and wavelength conversion in quantum dots," Physic. Review B, vol. 81, no. 3, pp. 035305, Jan. 2010.

[12] T. Akiyama, O. Wada, H. Kuwatsuka, T. Simoyama, Y. Nakata, K. Mukai, M. Sugawara, and H. Ishikawa, "Nonlinear processes responsible for nondegenerate four-wave mixing in quantum-dot optical amplifiers," Appl. Phys. Lett., vol. 77, no. 12, pp. 1753-1755, Sep. 2000.

[13] Z. G. Lu, J. R. Liu, S. Raymond, P. J. Barrios, D. Poitras, F. G. Sun, G. Pakulski, P. J. Bock, and T. Hall, "Highly efficient non-degenerate four-wave mixing process in InAs/InGaAsP quantum dots," Electon. Lett., vol. 42, no. 19, pp. 1112-1113, Sep. 2006.

[14] T. Akiyama, H. Kuwatsuka, N. Hatori, Y. Nakata, H. Ebe, and M. Sugawara, “Symmetric highly efficient (~0 dB) wavelength conversion based on four-wave mixing in quantum dot optical amplifiers,” IEEE Phonon. Technol. Lett. Vol. 14, no. 8, pp. 1139-1141, Aug. 2002.
[15] A. H. Flayyih, and A. H. Al-Khursan, “Four-wave mixing in quantum dot semiconductor optical amplifiers,” Applied Optics, vol. 52, no. 14, pp. 3156-3165, May. 2013.
[16] G. Yabre, “Effect of relatively strong light injection on the chirp-to-power ratio and the 3 dB bandwidth of directly modulated semiconductor lasers,” J. Lightwave Tech.,vol. 14, pp. 2367-2373, Oct. 1996.
[17] T. B. Simpson, J. M. Liu, and A. Gavrielides, “Bandwidth enhancement and broadband noise reduction in injection-locked semiconductor lasers,” IEEE Phonon. Technol. Lett., vol. 7, no. 7, pp. 709-711, Jul. 1995.
[18] X. J. Meng, T. Chau, and M. C. Wu, “Improved intrinsic dynamic distortions in directly modulated semiconductor lasers by optical injection locking,” IEEE Trans. Microw. Theory Tech., vol. 47, no. 7, pp. 1172-1176, Jul. 1999.
[19] N. A. Naderi, M. C. Pochet, F. Grillot, A. Shirkhorshidian, V. Kovanis, L. F. Lester, “Manipulation of the linewidth enhancement factor in an injection-locked quantum-dash Fabry-Perot laser at 1550 nm,” 23rd Annual Meeting of the IEEE Photonics Society, pp. 427-428, Nov. 2010.
[20] B. Lingnau, K. Ludge, W. W. Chow, E. Scholl, “Failure of the α factor in describing dynamical instabilities and chaos in quantum-dot lasers” Phys. Rev. E, vol. 86, no. 6, pp. 065201, Dec. 2012.
[21] C. H. Lin, and F. Y. Lin, “Four-wave mixing analysis on injection-locked quantum dot semiconductor lasers,” Opt. Express, vol. 21, no. 18, pp. 21242-21253, Sep. 2013.
[22] F. Lelarge et al., “Semiconductor lasers and optical amplifiers operating at 1.55 μm,” IEEE J. sel. Top. Quantum. Electron., vol. 13, no. 1, pp. 111-124, Jun. 2007.
[23] S. G. Li, Q. Gong, Y. F. Lao, H. D. Yang, S. Gao, P. Chen, Y. G. Zhang, S. L. Feng, and H. L. Wang, “Two-color quantum dot laser with tunable wavelength gap,” Appl. Phys. Lett., vol. 95, no. 25, pp. 251111-251113, Dec. 2009.
[24] T. H. Stievater, X. Q. Li, D. G. Steel, D. Gammon, D. S. Katzer, D. park, C. Piermarocchi, and L. J. Sham, “Rabi oscillations of excitons in single quantum dots,” Physic. Review Lett., vol. 87, no. 13, pp.133603-133606, Sep. 2001.
[25] P. Miska, J. Even, C. Paranthoen, and O. Dehaese, “Vertical electronic coupling between InAs/InP quantum-dot layers emitting in the near-infrared range,” Appl. Phys. Lett., vol. 86, no. 11, pp.111905-111907, Mar. 2005.
[26] C. Cornet, A. Schliwa, J. Even et al., “Electronic and optical properties of InAs/InP quantum dots on InP(100) and InP(311)B substrates: Theory and experiment,” Phys. Rev. B, vol.74, no. 3, pp. 3035312, Jul. 2006.
[27] R. Raghuraman, N. Yu, R. Engelmann, H. Lee, and C. L. Shieh, “Spectral dependence of differential gain, mode shift, and linewidth enhancement factor in a InGaAs-GaAs strained-layer single-quantum-well laser operated under high-injection conditions,” IEEE J. Quantum. Electron., vol. 29, no. 1, pp. 69-75, Jan. 1993.
[28] C. Cornet, C. Labbé, H. Folliot, N. Bertru, O. Dehaese, J. Even et al., “Quantitative investigation of optical absorption in InAs/InP (311)B quantum dots emitting at 1.55 μm wavelength,” Appl. Phys. Lett., vol. 85, no. 23, pp. 5685-5687, Oct. 2004.
[29] N. A. Naderi, M. Pochet, F. Grillot, N. B. Terry, V. Kovanis, and L. F. Lester, “Modeling the injection-locked behavior of a quantum dash semiconductor laser,” IEEE J. sel. Top. Quantum. Electron., vol. 15, no. 3, pp. 563-571, Jun. 2009.
[30] G. P. Agrawal, “Population pulsations and nondegenerate four-wave mixing in semiconductor lasers and amplifiers,” J. Opt. Soc. Am. B, vol. 5, no. 1, pp. 147-159, Jan.1988.
[31] K. Kikuchi, M. Kakui, C. E. Zah, and T. P. Lee, “Observation of highly nondegenerate four-wave mixing in 1.5 μm traveling-wave semiconductor optical amplifiers and estimation of nonlinear gain coefficient,” IEEE J. Quantum. Electron., vol. 28, no. 1, pp. 151-156, Jan.1992.
[32] I. Park, I. Fischer, and W. Elsaber, “Highly nondegenrate four-wave mixing in a tunable dual-mode semiconductor laser,” Appl. Phys. Lett., vol. 84, no. 25, pp. 5189-5191, Jun. 2004.
[33] I. Kolchanov, S. Kindt, K. Petermann, S. Diez, R. Ludwig, R. Schnabel, and H. G. Weber, “Analytical theory of terahertz four-wave mixing in semiconductor-laser amplifers,” Appl. Phys. Lett., vol. 68, no. 20, pp. 2787-2789, Mar. 1996.
[34] A. D’Ottavi, E. Iannone, A. mecozzi, S. Scotti, P. Spano, J. Landreau, A. Ougazzaden, and J. C. Bouley, “Investigation of carrier heating and spectral hole burning in semiconductor amplifiers by highly nondegenerate four-wave mixing,” Appl. Phys. Lett., vol. 64, no. 19, pp. 2492-2494, Feb. 1994.
[35] L. L. Li, and K. Petermann, “Small-signal analysis of THz optical-frequency conversion in an injection-locked semiconductor laser,” IEEE J. Quantum. Electron., vol. 29, no. 12, pp. 2988- 2994, Dec.1993.